 CMES, vol.4, no.6, pp.637-647, 2003

Application of Meshless Local Petrov-Galerkin (MLPG) Method to Elastodynamic Problems in Continuously Nonhomogeneous Solids

Jan Sladek[1], Vladimir Sladek[1] and Chuanzeng Zhang[2]

Abstract: A new computational method for solving transient elastodynamic initial-boundary value problems in continuously non-homogeneous solids, based on the meshless local Petrov-Galerkin (MLPG) method, is proposed in the present paper. The moving least squares (MLS) is used for interpolation and the modified fundamental solution as the test function. The local Petrov-Galerkin method for unsymmetric weak form in such a way is transformed to the local boundary integral equations (LBIE). The analyzed domain is divided into small subdomains, in which a weak solution is assumed to exist. Nodal points are randomly spread in the analyzed domain and each one is surrounded by a circle centered at the collocation point. The boundary-domain integral formulation with a static fundamental solution in Laplace transform domain is used to obtain the weak solution for subdomains. On the boundary of the subdomain, both the displacement and the traction vectors are unknown generally. If a modified fundamental solution vanishing on the boundary of the subdomain is employed, the traction vector is eliminated from the local boundary integral equations for all interior nodal points. The spatial variation of the displacements is approximated by the MLS scheme.

1 Introduction

The boundary integral equation method (BIEM) or boundary element method (BEM) is attractive mainly due to the possibility of reducing the dimensionality of a boundary value problem described by linear partial differential equations. To be successful in the reduction of the dimensionality it is needed to have the fundamental solution of the original partial differential equations available in an analytical or simple form. Different ways for solving the elastodynamic problems include the Laplace- and the Fourier-domain formulation [Manolis and Beskos (1988); Dominguez (1993); Sladek and Sladek (1984); Cruse and Rizzo (1968); Manolis and Beskos (1981)], time-domain formulation [Cole et al. (1978); Mansur (1983); Schanz and Antes (1997)], and the mass matrix approach with domain discretization [Nardini and Brebbia (1983); Chirino et al. (1994); Fedelinski et al. (1993); Perez-Gavilan and Aliabadi (2000); Kögl and Gaul (2000)]. In the time-domain formulation, both spatial and temporal discretizations are required. The fundamental solution in such a case is quite complicated. It increases computational time for the numerical evaluation of integrals. In the Laplace-transform domain formulation, the fundamental solution is also complex and several quasi-static boundary value problems are to be solved for various values of the Laplace transform parameter. In the mass matrix formulation the static fundamental solution is utilized. However, it leads to a boundary-domain integral formulation, because the static fundamental solution is not the solution of the elastodynamic governing equations. The domain-integral of inertia terms can be transformed into boundary integrals by the dual reciprocity method [Partrige et al. (1992); Beskos (1997)]. For a better spatial approximation, additional interior nodes to the boundary ones are required. However, if interior nodes are spread in the domain it is convenient to use a meshless approximation.

The elastodynamic fundamental solution is available in the time- and Laplace-transform-domain for a homogeneous solid [Dominguez (1993)]. For exponentially graded non-homogenoeus solids, elastostatic fundamental solutions have been derived by Martin et al. (2002) and Chan et al. (2003). A free-space Green's function for problems involving time-harmonic elastic waves in variable density materials under plane strain conditions has been developed by Manolis and Pavlou (2002). They used the Hormander method in context of matrix algebra formalism. For exponentially graded nonhomogenoeus

[1] Institute of Construction and Architecture, Slovak Academy of Sciences, 84503 Bratislava, Slovakia, email: usarslad@savba.sk

[2] Department of Civil Engineering, University of Applied Sciences Zittau/Görlitz, D-02763 Zittau, Germany, email: c.zhang@hs-zigr.de

solids, Fourier-integral representations of elastostatic and elastodynamic fundamental solutions have been applied by Zhang et al. (2003a, 2003b) for elastostatic and elastodynamic crack analysis in FGMs. Since no elastostatic and elastodynamic fundamental solutions are yet available for general FGMs, one can use alternatively in a general nonhomogeneous case a parametrix (Levi function) instead of the fundamental solutions [Mikhailov (2002)]. Parametrix correctly describes the main part of the fundamental solution but is not required to satisfy the original differential equations.

In the present analysis the meshless local Petrov-Galerkin (MLPG) method [Atluri et al. (1998, 1999); Atluri and Shen (2002a,b)] is used to solve transient elastodynamic problems in continuously nonhomogeneous solid. The modified elastostatic fundamental solution or the parametrix on a circular subdomain is used as the test function in the MLPG method for unsymmetric weak form. Fundamental solution corresponds to a homogeneous case with material parameters at the center of circular subdomain.. It is leading to a local boundary-domain integral formulation. Formally, it is very similar to boundary-domain integral formulations, which were derived for nonlinear problems solved by local boundary integral equation (LBIE) method [Zhu et al. (1998b, 1999)]. In this method, small subdomains covering the analyzed domain are introduced. On the boundary of the subdomains (artificial boundary) lying in the interior of the body, both the displacement and the traction vectors are unknown. To eliminate the number of unknowns, either the parametrix or the corresponding fundamental traction vector should vanish on the boundary of the subdomains. Different methods can be used to obtain a parametrix vanishing on the boundary of the subdomains. Methods based on a companion solution [Zhu et al. (1998a); Sladek et al. (2000)] and on the cut-off functions are applied in the present paper. Laplace-transform is used to convert the hyperbolic elastodynamic governing equations into elliptic partial differential equations. Local boundary integral equations (LBIEs) are given in the Laplace-transform domain and applied to small subdomains. In such a case, the LBIEs involve a domain-integral representing the dynamic terms resulting from the inertia term and the initial values. There are no problems with numerical integration of this domain-integral when the MLS approximation is employed for the spatial variation of the unknown boundary data. Several quasi-static boundary value problems have to be solved for various values of the Laplace transform parameter. The Stehfest inversion method [Stehfest (1970)] is applied to obtain the time-dependent values.

Numerical examples are presented to show the accuracy of the proposed local boundary integral equation method (LBIEM).

2 Local boundary integral equations

Consider an isotropic, non-homogeneous and linear elastic solid with Young's modulus $E(\mathbf{x})$ being dependent on Cartesian coordinates and the Poisson's ratio ν being constant. Under these assumptions we can write the elasticity tensor as

$$c_{ijkl}(\mathbf{x}) = \mu(\mathbf{x}) c^0_{ijkl} \quad \text{with} \quad \mu(\mathbf{x}) = \tfrac{E(\mathbf{x})}{2(1+\nu)},$$

$$c^0_{ijkl} = 2\nu/(1-2\nu)\delta_{ij}\delta_{kl} + \delta_{ik}\delta_{jl} + \delta_{il}\delta_{jk}\,. \tag{1}$$

In eq. (1), $\mu(\mathbf{x})$ represents the shear modulus, and δ_{ij} denotes the Kronecker delta. The equations of motion in terms of displacements in a non-homogeneous solid have the following form

$$\mu u_{i,kk} + \frac{\mu}{1-2\nu} u_{k,ki} = -X_i - \mu_{,i}\frac{2\nu}{1-2\nu} u_{k,k} - \mu_{,j}(u_{i,j} + u_{j,i}) + \rho\ddot{u}_i\,, \tag{2}$$

where u_i and X_i are the components of the time-dependent displacement and body force vectors, and ρ is the mass density of the material, respectively. Also, a comma after a quantity represents spatial derivatives, while dots indicate differentiations with respect to time.

Applying the Laplace transform to the equations of motion (2), we obtain

$$\mu\overline{u}_{i,kk} + \frac{\mu}{1-2\nu}\overline{u}_{k,ki} + \overline{F}_i + \overline{g}_i - \rho p^2 \overline{u}_i = 0\,, \tag{3}$$

where

$$\overline{g}_i(\mathbf{x},p) = \mu_{,i}(\mathbf{x})\frac{2\nu}{1-2\nu}\overline{u}_{k,k}(\mathbf{x},p) - \mu_{,j}(\mathbf{x})\left[\overline{u}_{i,j}(\mathbf{x},p) + \overline{u}_{j,i}(\mathbf{x},p)\right], \quad \text{and}$$

$$\overline{F}_i(\mathbf{x},p) = \overline{X}_i(\mathbf{x},p) + p u_i(\mathbf{x}) + \dot{u}_i(\mathbf{x})$$

is a redefined body force vector in the Laplace-transformed domain with the initial boundary conditions

for the displacements $u_i(\mathbf{x})$ and velocities $\dot{u}_i(\mathbf{x})$, and p is the Laplace transform parameter.

Following the derivation of the boundary-domain formulation for elastostatic boundary value problems in nonhomogeneous media [Sladek et al. (1993)], we can obtain the integral identity

$$\int_\Omega \left\{ \overline{u}_{i,kk}(\mathbf{x},p) + \frac{1}{1-2\nu}\overline{u}_{k,ki}(\mathbf{x},p) + \frac{1}{\mu(\mathbf{x})}\left[\overline{F}_i(\mathbf{x},p) + \overline{g}_i(\mathbf{x},p) - \rho p^2 \overline{u}_i(\mathbf{x},p)\right] \right\} U_{ij}(\mathbf{x},\mathbf{y}) d\Omega = 0 \quad , \tag{4}$$

where $U_{ij}(\mathbf{x},\mathbf{y})$ stand for the displacement fundamental solutions in an elastic medium with $\mu = 1$. Applying the Gauss divergence theorem to the domain integral in eq. (4), we obtain

$$\int_\Omega \left[U_{ij,kk}(\mathbf{x},\mathbf{y}) + \frac{1}{1-2\nu} U_{kj,ki}(\mathbf{x},\mathbf{y}) \right] \overline{u}_i(\mathbf{x},p) d\Omega + \int_\Gamma \left[\frac{1}{\mu(\mathbf{x})} \overline{t}_i(\mathbf{x},p) U_{ij}(\mathbf{x},\mathbf{y}) - T_{ij}(\mathbf{x},\mathbf{y}) \overline{u}_i(\mathbf{x},p) \right] d\Gamma = \int_\Omega \frac{1}{\mu(\mathbf{x})} \left[\rho p^2 \overline{u}_i(\mathbf{x},p) - \overline{F}_i(\mathbf{x},p) - \overline{g}_i(\mathbf{x},p) \right] U_{ij}(\mathbf{x},\mathbf{y}) d\Omega, \tag{5}$$

where

$$\overline{t}_i(\mathbf{x},p) = \mu(\mathbf{x})\overline{u}_{i,k}(\mathbf{x},p) n_k + \mu(\mathbf{x}) \frac{2\nu}{1-2\nu} \overline{u}_{k,k}(\mathbf{x},p) n_i + \mu(\mathbf{x}) \overline{u}_{k,i}(\mathbf{x},p) n_k \tag{6}$$

is the traction vector with the unit outward normal vector n_i to the boundary Γ. The traction fundamental solutions are defined as

$$T_{ij}(\mathbf{x},\mathbf{y}) = \frac{2\nu}{1-2\nu} U_{kj,k}(\mathbf{x},\mathbf{y}) n_i(\mathbf{x}) + U_{ij,k}(\mathbf{x},\mathbf{y}) n_k(\mathbf{x}) + U_{kj,i}(\mathbf{x},\mathbf{y}) n_k(\mathbf{x}) .$$

Since

$$U_{ij,kk}(\mathbf{x},\mathbf{y}) + \frac{1}{1-2\nu} U_{kj,ki}(\mathbf{x},\mathbf{y}) = -\delta_{ij}\delta(\mathbf{x}-\mathbf{y}) , \tag{7}$$

the integral identity (5) yields the integral representation for the displacements

$$\overline{u}_j(\mathbf{y},p) = \int_\Gamma \frac{1}{\mu(\mathbf{x})} \overline{t}_i(\mathbf{x},p) U_{ij}(\mathbf{x},\mathbf{y}) d\Gamma - \int_\Gamma T_{ij}(\mathbf{x},\mathbf{y}) \overline{u}_i(\mathbf{x},p) d\Gamma + \int_\Omega \frac{1}{\mu(\mathbf{x})} \left[\overline{F}_i(\mathbf{x},p) + \overline{g}_i(\mathbf{x},p) - \rho p^2 \overline{u}_i(\mathbf{x},p) \right] U_{ij}(\mathbf{x},\mathbf{y}) d\Omega . \tag{8}$$

The integro-differential equations (8) have to be supplemented by the integral representation for displacement gradients in order to get the complete boundary-domain formulation [Sladek et al. (1993)]. If, instead of the entire domain Ω of the given problem, we consider a subdomain Ω_s, which is located entirely inside Ω, the following local boundary integral equations (LBIEs) should also be valid over the sub-domain

$$\overline{u}_j(\mathbf{y},p) = \int_{\partial\Omega_s} \frac{1}{\mu(\mathbf{x})} \overline{t}_i(\mathbf{x},p) U_{ij}(\mathbf{x},\mathbf{y}) d\Gamma - \int_{\partial\Omega_s} T_{ij}(\mathbf{x},\mathbf{y}) \overline{u}_i(\mathbf{x},p) d\Gamma + \int_{\Omega_s} \frac{1}{\mu(\mathbf{x})} \left[\overline{F}_i(\mathbf{x},p) + \overline{g}_i(\mathbf{x},p) - \rho p^2 \overline{u}_i(\mathbf{x},p) \right] U_{ij}(\mathbf{x},\mathbf{y}) d\Omega , \tag{9}$$

where $\partial\Omega_s$ is the boundary of the sub-domain Ω_s.

Both the displacement and the traction vectors are unknown on the artificial boundary $\partial\Omega_s$. If the fundamental solution $U_{ij}(\mathbf{x},\mathbf{y})$ were vanishing on the boundary of the sub-domain, the integral containing the traction vector could be eliminated. This can be realized in two ways. The first one, more general for a wide class of partial of differential equations, is based on the use of cut-off functions [Mikhailov (2002)]. The parametrix P_{ij} for a circular sub-domain with a radius r_0 can be written in the following form

$$P_{ij}(\mathbf{x},\mathbf{y}) = \chi(r) U_{ij}(\mathbf{x},\mathbf{y}) , \tag{10}$$

where the cut-off function $\chi(r)$ can be selected as

$$\chi(r) = 1 - \frac{r^2}{r_0^2} \text{ with } r = |\mathbf{x}-\mathbf{y}| .$$

If the displacement fundamental solutions are replaced by the parametrix P_{ij}, one obtains an integral representation for the displacements in the Laplace transformed domain

$$\begin{aligned}
&\overline{u}_j(\mathbf{y},p)\\
&=\int_{\partial\Omega_s}\frac{1}{\mu(\mathbf{x})}\overline{t}_i(\mathbf{x},p)P_{ij}(\mathbf{x},\mathbf{y})d\Gamma\\
&-\int_{\partial\Omega_s}\overline{u}_k(\mathbf{x},p)n_l(\mathbf{x})c^o_{klim}P_{ij,m}(\mathbf{x},\mathbf{y})d\Gamma\\
&+\int_{\Omega_s}\left\{\frac{1}{\mu(\mathbf{x})}\left[\overline{F}_i(\mathbf{x},p)+\overline{g}_i(\mathbf{x},p)-\rho p^2\overline{u}_i(\mathbf{x},p)\right]P_{ij}(\mathbf{x},\mathbf{y})\right.\\
&+\overline{u}_k(\mathbf{x})c^o_{klim}\left[\chi_{,l}(r)U_{ij,m}(\mathbf{x},\mathbf{y})+\chi_{,m}(r)U_{ij,l}(\mathbf{x},\mathbf{y})\right.\\
&\left.\left.+\chi_{,ml}(r)U_{ij}(\mathbf{x},\mathbf{y})\right]\right\}d\Omega \quad . \qquad (11)
\end{aligned}$$

Bearing in mind that $\chi(r)|_{\partial\Omega_s}=0$, we may rewrite the integral representation (11) as

$$\begin{aligned}
&\overline{u}_j(\mathbf{y},p)\\
&=-\int_{\partial\Omega_s}\overline{u}_k(\mathbf{x},p)N_{kj}(\mathbf{x},\mathbf{y})d\Gamma\\
&+\int_{\Omega_s}\left\{\frac{1}{\mu(\mathbf{x})}\left[\overline{F}_i(\mathbf{x},p)+\overline{g}_i(\mathbf{x},p)-\rho p^2\overline{u}_i(\mathbf{x},p)\right]P_{ij}(\mathbf{x},\mathbf{y})\right.\\
&\left.+\overline{u}_k(\mathbf{x})M_{kj}(\mathbf{x},\mathbf{y})\right\}d\Omega \qquad (12)
\end{aligned}$$

where

$$N_{kj}(\mathbf{x},\mathbf{y})=U_{ij}(\mathbf{x},\mathbf{y})n_l(\mathbf{x})c^o_{klim}\chi_{,m}(r),$$

$$\begin{aligned}
M_{kj}(\mathbf{x},\mathbf{y})=c^o_{klim}&\left[\chi_{,l}(r)U_{ij,m}(\mathbf{x},\mathbf{y})+\chi_{,m}(r)U_{ij,l}(\mathbf{x},\mathbf{y})\right.\\
&\left.+\chi_{,ml}(r)U_{ij}(\mathbf{x},\mathbf{y})\right] \quad .
\end{aligned}$$

The other way for the elimination of tractions on $\partial\Omega_s$ is based on the use of a companion solution [Sladek et al. (2003)]. The companion solution $\tilde{U}_{ij}$ is associated with the elastostatic fundamental solution U_{ij} and is defined as the solution to the following equations

$$\begin{aligned}
&c_{imkl}\tilde{U}_{kj,lm}=0 \quad \text{on} \quad \Omega'_s \quad ,\\
&\tilde{U}_{ij}=U_{ij} \quad \text{on} \quad \partial\Omega'_s \quad , \qquad (13)
\end{aligned}$$

where Ω'_s is a circle of the radius r_0, which coincides with Ω_s for interior points. The modified fundamental solution $U^*_{ij}=U_{ij}-\tilde{U}_{ij}$ has to satisfy the governing equation (7). On the boundary of the circle $\partial\Omega'_s$, this fundamental solution is zero due to the second condition in (13). Hence, we can rewrite eq. (9) as

$$\begin{aligned}
\overline{u}_j(\mathbf{y},p)=&-\int_{\partial\Omega_s}T^*_{ij}(\mathbf{x},\mathbf{y})\overline{u}_i(\mathbf{x},p)d\Gamma\\
&+\int_{\Omega_s}\frac{1}{\mu(\mathbf{x})}\left[\overline{F}_i(\mathbf{x},p)+\overline{g}_i(\mathbf{x},p)-\rho p^2\overline{u}_i(\mathbf{x},p)\right]U^*_{ij}(\mathbf{x},\mathbf{y})d\Omega \qquad (14)
\end{aligned}$$

for the source point $\mathbf{y}$ located inside Ω. The explicit expression for the modified fundamental solutions U^*_{ij} and T^*_{ij} can be found in [Atluri et al. (2000)].

For a source point located on the global boundary $\zeta\in\Gamma_s\subset\Gamma$ the LBIEs can be written as

$$\begin{aligned}
&\overline{u}_j(\zeta,p)+\int_{L_s}T^*_{ij}(\mathbf{x},\zeta)\overline{u}_i(\mathbf{x},p)d\Gamma+\\
&\lim_{\mathbf{y}\to\zeta}\int_{\Gamma_s}T^*_{ij}(\mathbf{x},\mathbf{y})\overline{u}_j(\mathbf{x},p)d\Gamma-\int_{\Gamma_s}\frac{1}{\mu(\mathbf{x})}\overline{t}_i(\mathbf{x},p)U^*_{ij}(\mathbf{x},\zeta)d\Gamma\\
&=\int_{\Omega_s}\frac{1}{\mu(\mathbf{x})}\left[\overline{F}_i(\mathbf{x},p)+\overline{g}_i(\mathbf{x},p)-\rho p^2\overline{u}_i(\mathbf{x},p)\right]U^*_{ij}(\mathbf{x},\zeta)d\Omega. \qquad (15)
\end{aligned}$$

The LBIEs (14) and (15) with modified fundamental solutions have a simpler form in elastodynamics than the previous one (12) with a parametrix utilizing a continuous cut-off function.

3 Numerical solution method of local boundary integral equations

Unlike the conventional numerical solution procedures such as the dual reciprocity method, a meshless method is presented in this section to solve the boundary-domain LBIEs (15). The present meshless method is based on a moving least squares (MLS) approximation, which is generally considered as one of many schemes to interpolate discrete data with a reasonable accuracy. The approximated function can be written as [Belytschko et al. (1996)]

$$\overline{\mathbf{u}}(\mathbf{x},p)=\mathbf{\Phi}^T(\mathbf{x})\hat{\mathbf{u}}=\sum_{j=1}^{n}\phi_j(\mathbf{x})\hat{\mathbf{u}}_j(p)\,, \qquad (16)$$

where $\hat{\mathbf{u}}_j(p)$ are fictitious parameters and $\phi_j(\mathbf{x})$ is the shape function associated with node j. Substituting the MLS approximation (16) into eq. (6) we obtain for the traction vector

$$\bar{\mathbf{t}}(\mathbf{x},p)=\mathbf{N}(\mathbf{x})\mathbf{D}\sum_{j=1}^{n}B_j(\mathbf{x})\hat{\mathbf{u}}_j(p)\,, \tag{17}$$

where the matrix $\mathbf{N}(\mathbf{x})$ corresponds to the normal vector at $\mathbf{x}$, $\mathbf{D}$ is the stress-strain matrix and the matrix $B_j(\mathbf{x})$ represents the gradients of the shape functions at $\mathbf{x}$.

Let $\Gamma_s=\Gamma_{su}\cup\Gamma_{st}$, where Γ_{su} and Γ_{st} are parts of Γ_s over which the displacements and the tractions are prescribed, respectively. Making use of the MLS approximations (16) and (17), the LBIEs (14) and (15) are converted into a set of linear algebraic equations as

$$\begin{aligned}&\sum_{j=1}^{n}\left\{\phi_j(\mathbf{y}_i)+\int_{\partial\Omega_s}\mathbf{T}^*(\mathbf{x},\mathbf{y}_i)\phi_j(\mathbf{x})d\Gamma\right\}\hat{\mathbf{u}}_j(p)\\&=\int_{\Omega_s}\frac{1}{\mu(\mathbf{x})}\mathbf{U}^*(\mathbf{x},\mathbf{y}_i)\mathbf{F}(\mathbf{x})d\Omega\\&-\sum_{j=1}^{n}\int_{\Omega_s}\frac{1}{\mu(\mathbf{x})}\mathbf{U}^*(\mathbf{x},\mathbf{y}_i)\left(\rho(\mathbf{x})p^2\phi_j(\mathbf{x})-\mathbf{G}_j(\mathbf{x})\right)d\Omega\,\hat{\mathbf{u}}_j(p)\end{aligned} \tag{18}$$

for $\mathbf{y}_i\in\Omega$, and

$$\begin{aligned}&\sum_{j=1}^{n}\left\{\phi_j(\zeta_i)+\lim_{y\to\zeta_i}\int_{\Gamma_{st}}\mathbf{T}^*(\mathbf{x},\mathbf{y})\phi_j(\mathbf{x})d\Gamma\right.\\&+\int_{L_s}\mathbf{T}^*(\mathbf{x},\zeta_i)\phi_j(\mathbf{x})d\Gamma\\&\left.-\int_{\Gamma_{su}}\frac{1}{\mu(\mathbf{x})}\mathbf{U}^*(\mathbf{x},\zeta_i)\mathbf{N}(\mathbf{x})\mathbf{D}B_j(\mathbf{x})\right\}\hat{\mathbf{u}}_j(p)\\&=\int_{\Gamma_{st}}\frac{1}{\mu(\mathbf{x})}\mathbf{U}^*(\mathbf{x},\zeta_i)\tilde{\mathbf{t}}(\mathbf{x})d\Gamma\\&-\int_{\Gamma_{su}}\mathbf{T}^*(\mathbf{x},\zeta_i)\tilde{\mathbf{u}}(\mathbf{x})d\Gamma+\int_{\Omega_s}\frac{1}{\mu(\mathbf{x})}\mathbf{U}^*(\mathbf{x},\zeta_i)\mathbf{F}(\mathbf{x})d\Omega\\&-\sum_{j=1}^{n}\int_{\Omega_s}\frac{1}{\mu(\mathbf{x})}\mathbf{U}^*(\mathbf{x},\zeta)\left(\rho(\mathbf{x})p^2\phi_j(\mathbf{x})-\mathbf{G}_j(\mathbf{x})\right)d\Omega\,\hat{\mathbf{u}}_j(p)\end{aligned} \tag{19}$$

for $\zeta_i\in\Gamma_s$, where

$$\mathbf{G}_j(\mathbf{x})=\begin{bmatrix}2\frac{1-\nu}{1-2\nu}\mu_{,1}\phi_{j,1}+\mu_{,2}\phi_{j,2}\,; & \frac{2\nu}{1-2\nu}\mu_{,1}\phi_{j,2}+\mu_{,2}\phi_{j,1}\\ \frac{2\nu}{1-2\nu}\mu_{,2}\phi_{j,1}+\mu_{,1}\phi_{j,2}\,; & 2\frac{1-\nu}{1-2\nu}\mu_{,2}\phi_{j,2}+\mu_{,1}\phi_{j,1}\end{bmatrix}$$

and L_s is the circular part of $\partial\Omega_s$ and $\Gamma_s=\partial\Omega_s-L_s$, if the collocation point lies on the global boundary, $\mathbf{y}\in\partial\Omega$ [Sladek et al. (2001)]. In eqs. (18) and (19), the matrix notations $\mathbf{U}^*$, $\mathbf{T}^*$ are used instead of the index notations U^*_{ij} and T^*_{ij}, and the prescribed boundary data are denoted as $\tilde{\mathbf{u}}$ and $\tilde{\mathbf{t}}$, respectively.

The time-dependent values of the transformed quantities in the previous consideration can be obtained by an inverse transform. There are many inversion methods available for the inverse Laplace transform. As the inverse Laplace transform is an ill-posed problem, small truncation errors can be greatly magnified in the inversion process and hence lead to poor numerical results. In the present analysis, the sophisticated Stehfest's algorithm [Stehfest (1970)] for the numerical inversion is used. If $\overline{f}(p)$ is the Laplace transform of $f(t)$, an approximate value f_a of $f(t)$ for a specific time t is given by

$$f_a(t)=\frac{\ln 2}{t}\sum_{i=1}^{N}v_i\,\overline{f}\left(\frac{\ln 2}{t}i\right)\quad, \tag{20}$$

where

$$v_i=(-1)^{N/2+i}\sum_{k=[(i+1)/2]}^{\max(i,N/2)}\frac{k^{N/2}(2k)!}{(N/2-k)!\,k!\,(k-1)!\,(i-k)!\,(2k-i)!}\quad. \tag{21}$$

Sutradhar et al. (2002) have suggested to use N = 10 for single precision arithmetic. It means that for each time t it is needed to solve N boundary value problems for the corresponding Laplace parameters $p=i\ln 2/t$, with $i=1,2,...,N$. If M denotes the number of the time instants in which we are interested to know $f(t)$, the number of the required Laplace transform solutions $\overline{f}(p_j)$ is then $M\times N$. Most of the methods for the numerical inversion of the Laplace transform require the use of complex-valued Laplace transform parameter, and as a result, the

application of complex arithmetic may lead to additional storage requirement and an increase in computing time. A critical study of various inversion algorithms is given by Davies and Martin (1979).

4 Numerical examples

4.1 A nonhomogeneous elastic strip

As the first numerical example, a nonhomogeneous elastic strip as depicted in Fig. 1 is considered. The strip is subjected to an impact traction loading $t_1 = 10H(\tau - 0)$ at the end $x_1 = L$, while the opposite end is fixed in the x_1-direction. The other boundaries are free of tractions. Here, $H(\tau\text{-}0)$ is the Heaviside unit step function. The length of the strip is L = 10 and the width w = 2. Young's modulus varies linearly according to

$$E(x_1) = E_0 + (x_1 - L/2)\gamma E_0 . \tag{22}$$

The material parameters used in the calculation are: Young's modulus $E_0 = 10^4$, nonhomogeneity parameter $\gamma = 0.1$, Poisson's ratio $\nu = 0.2$, and mass density $\rho = 1$. In Fig. 2, the numerical results obtained by the present LBIEM are compared with the FEM results provided by the NASTRAN code. In the FEM analysis the domain is discretized by 80 linear elements and 6000 time steps.

In the LBIEM, 48 boundary nodes and additional 57 internal nodes with a regular distribution is used, see Fig. 1. For the inverse Laplace transform, the Stehfest algorithm is applied. The time variation of the displacement component u_1 at the mid of the strip, i.e., $x_1 = L/2$ and $x_2 = w/2$, is shown in Fig. 2 for $\gamma = 0.1$. One can observe in Fig. 2 a quite good agreement between both numerical results. This confirms the accuracy and the reliability of the present LBIEM. The time variation of the traction vector at the fixed end $x_1 = 0$, is shown in Fig. 3. Again a good agreement of both numerical results is obtained.

The influence of the nonhomogeneity parameter on the time variation of the displacement component u_1 is presented in Fig. 4. Before the first wave arrival at the mid of the strip, the displacement is zero. The velocity of wave propagation is changing in a continuously nonhomogeneuos strip. The largest value of the displacement is expected when the reflected wave is interfering with the initial incident wave. With increasing value of the nonhomogeneity parameter γ the absolute value of the first pick of the displacement u_1 increases. The time variation of the displacement component u_1 corresponding to

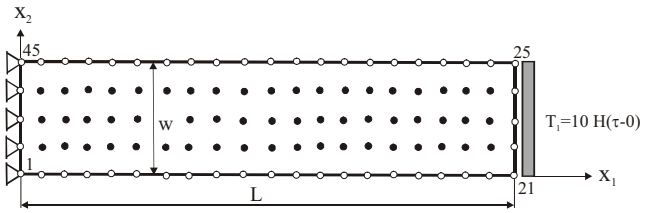

Figure 1 : A nonhomogeneous elastic strip subjected to an impact loading

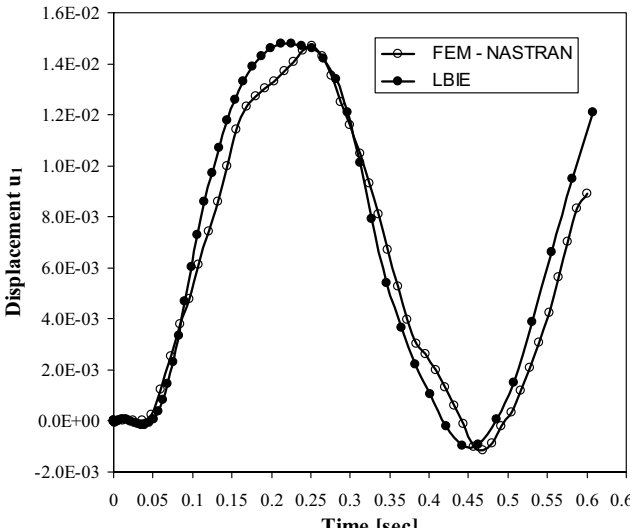

Figure 2 : Time variation of the displacement component u_1 at the mid of the nonhomogeneous strip with the parameter $\gamma = 0.1$

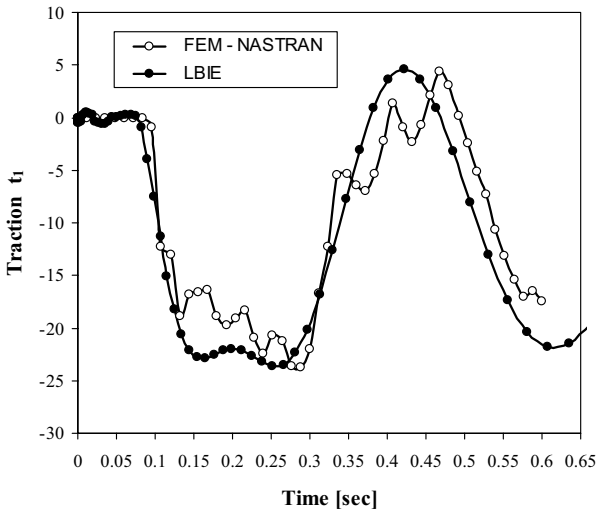

Figure 3 : Time variation of the traction component t_1 at the fixed end of the nonhomogeneous strip

Table 1 : Relative errors for radial displacements and hoop stresses in a homogeneous hollow cylinder under a static load

Radial coordinate	Radial displacements			Hoop stresses		
	Analytical	LBIEM	Relative errors	Analytical	LBIEM	Relative errors
r = a	$3,8044\ 10^{-3}$	$3,774\ 10^{-3}$	0,008	4,555	4,501	0,0118
r = b	$3,5555\ 10^{-3}$	$3,573\ 10^{-3}$	0,0049	3,555	3,587	0,009

a homogeneous strip is presented by a solid line without symbols in Fig. 4.

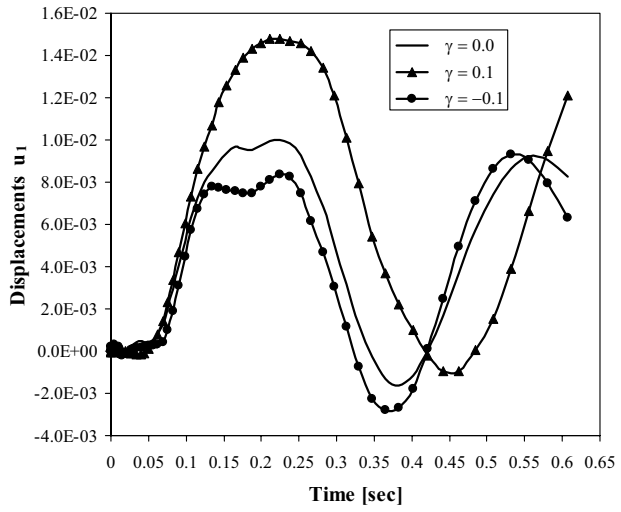

Figure 4 : Time variation of the displacement component u_1 at the mid of the strip for three different values of the nonhomogeneity parameter γ

4.2 An infinitely long hollow cylinder

In the second numerical example, an infinitely long hollow cylinder with a radial exponential variation of Young's modulus is considered

$$E(r) = E_0 \exp(\gamma(r-a)), \tag{23}$$

where $E_0 = 10^4$, Poisson ratio is considered to be constant $\nu = 0.2$, and the mass density is constant too $\rho = 1$. The inner and outer radii of the hollow cylinder are taken as $a = 8$ and $b = 10$, respectively. A uniform pressure $p = 1$ is acting on the inner surface of the cylinder. Due to the axial symmetry of the problem it is sufficient to analyze only one quarter of the cylinder. In the LBIEM 84 nodes are used for the MLS approximation of the displacements. A regular distribution of nodes with 42 boundary nodes is considered, see Fig. 5. To test the accuracy of the present method a homogeneous hollow cylinder, i.e., $\gamma = 0$, and a static load are considered in the first step. Numerical results for the radial displacements and the hoop stresses are compared with the following analytical solutions

$$u_r = \frac{pr}{(b/a)^2 - 1} \frac{1}{E_0} \left[(1+\nu) \left(\frac{b}{r} \right)^2 + 1 - \nu \right], \tag{24}$$

$$\sigma_{\varphi\varphi} = \frac{p}{(b/a)^2 - 1} \left[\left(\frac{b}{r} \right)^2 + 1 \right]. \tag{25}$$

One can observe in Tab. 1 that the relative errors for the radial displacements are less than 0,8% and for the hoop stresses less than 1,18%.

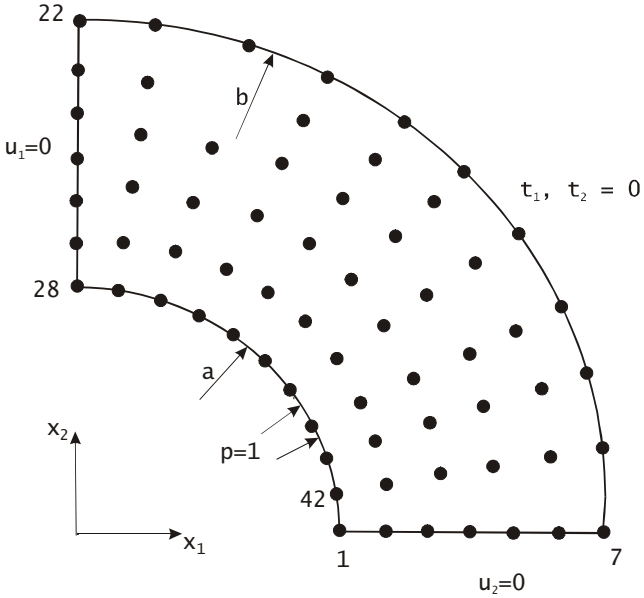

Figure 5 : Node distribution in a quarter of the hollow cylinder under a pressure load on the inner surface

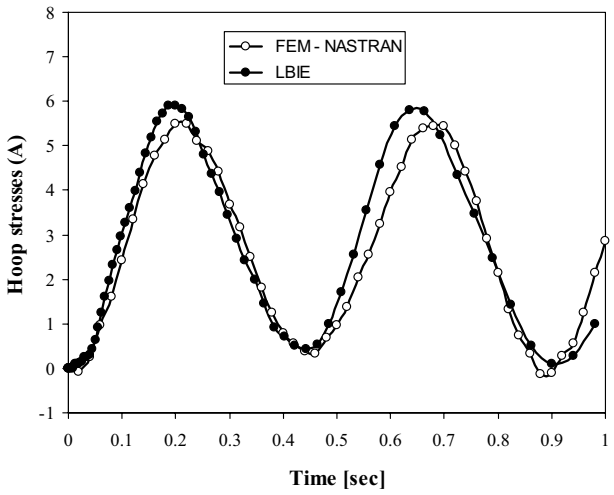

Figure 7 : Time variation of the hoop stress on the inner surface of a nonhomogeneous hollow cylinder with $\gamma = 0.5$

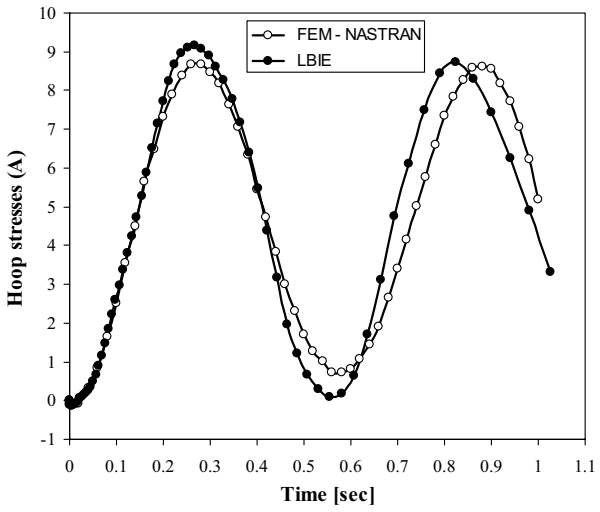

Figure 6 : Time variation of the hoop stress on the inner surface of a homogeneous hollow cylinder

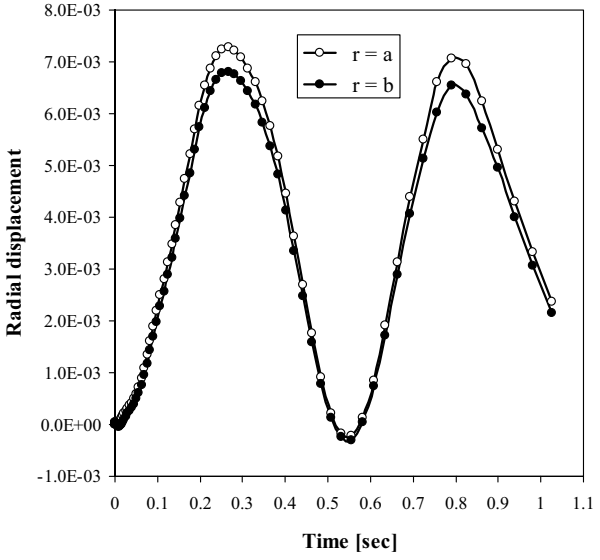

Figure 8 : Time variation of radial displacements on the inner and outer surfaces of the nonhomogeneous cylinder

The numerical results corresponding to a uniform impact pressure load on the inner surface of the hollow cylinder are compared with those obtained by the FEM analysis, where the domain is discretized by 576 linear elements and 6000 time steps are used for the time approximation. The hoop stresses at the inner radius (point A) are given in Fig. 6. One can observe a good agreement of both results.

Next, a nonhomogeneous cylinder with $\gamma = 0.5$ is analyzed. The same node distribution as in the previous numerical example is used. The hoop stresses at point A are compared with FEM results in Fig. 7. The time

variations of the radial displacements on inner and outer surfaces of the cylinder are shown in Fig. 8. The time variations on both surfaces are very similar. The maximum values of the radial displacements are reached at the same instants.

The time variations of the hoop stresses on both inner and outer surfaces of the nonhomogeneous hollow cylinder are presented in Fig. 9, which shows that the peak hoop stress on the inner surface is larger than that on the outer surface of the hollow cylinder. The influence of the material nonhomogeneity parameter γ on the time variation of the hoop stress at point A is shown in Fig. 10. It can be seen from Fig. 10 that the peak hoop stress at the same point on the inner surface of the hollow cylinder is reduced as the nonhomogeneity parameter γ increases, which is favourable from the mechanics points of view.

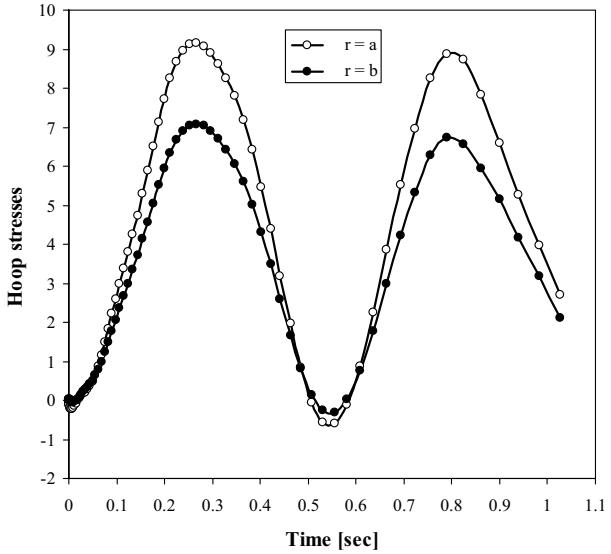

Figure 9 : Time variation of hoop stresses on both inner and outer surfaces of the nonhomogeneous cylinder

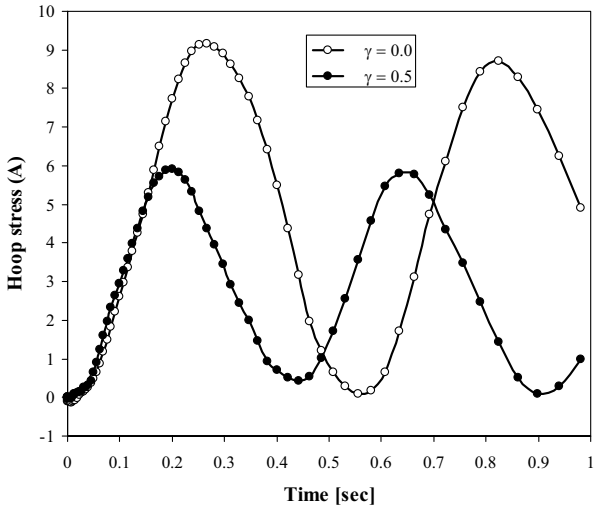

Figure 10 : Comparison of the time variations of the hoop stresses on the inner surface of the homogeneous and nonhomogeneous hollow cylinders

5 Conclusion

A local boundary integral equation formulation in Laplace-transform domain with a meshless approximation has been successfully implemented to solve 2-d initial-boundary value problems in transient elastodynamics for continuously nonhomogeneous solids. The static fundamental solution is used to derive the boundary-domain integral formulation. The analysed domain is divided into small no-overlapping circular subdomains to which the local boundary integral equations are applied. The limitation of the conventional boundary element approaches to homogeneous solids is removed by using the present LBIEM. The computational accuracy of the present LBIEM is comparable with that of FEM. However, the versatility and the adaptability of the present LBIEM are higher than in the conventional FEM.

Acknowledgement: The authors acknowledge the support by the Slovak Science and Technology Assistance Agency registered under number APVT-51-003702, as well as by the Slovak Grant Agency VEGA – 2303823, and the Project for Bilateral Cooperation in Science and Technology supported jointly by the International Bureau of the German BMBF and the Ministry of Education of Slovak Republic under the project number SVK 01/020.

References

Atluri, S. N.; Sladek, J.; Sladek, V.; Zhu, T. (2000): The local boundary integral equation (LBIE) and its meshless implementation for linear elasticity. *Comput. Mech.*, 25: 180-198.

Atluri, S. N.; Zhu, T. (1998): A new meshless local Petrov-Galerkin (MLPG) approach in computational mechanics. *Comput. Mech.*, 22: 117-127.

Atluri, S. N.; Him, H. G.; Cho, C. Y. (1999): A critical assessment of the truly meshless local Petrov-Galerkin (MLPG) and local boundary integral equation (LBIE) methods. *Comput. Mech.*, 24: 348-372.

Atluri, S. N.; Shen, S. P. (2002a): The meshless local Petrov-Galerkin (MLPG) method: A simple & less-costly alternative to the finite element and boundary element methods. *CMES: Computer Modeling in Engineering & Sciences*, 3: 11-51.

Atluri, S. N.; Shen, S. P. (200b): The Meshless Local Petrov-Galerkin (MLPG) Method, Tech. Science Press.

Balas, J.; Sladek, J.; Sladek, V. (1989): Stress Analysis by Boundary Element Methods, Elsevier, Amsterdam.

Belytschko, T.; Krongauz, Y.; Organ, D.; Fleming, M.; Krysl, P. (1996): Meshless methods; An overview and recent developments. *Comp. Meth. Appl. Mech. Engn.*, 139: 3-47.

Beskos, D. (1997): Boundary element methods in dynamic analysis II. *Appl. Mech. Rev.*, 40: 1-23.

Chan, Y.-S.; Gray, L. J.; Kaplan, T.; Paulino, G. H. (2003): Green's function for a two-dimensional exponentially-graded elastic medium. Submitted for publication.

Chirino, F.; Gallego, R.; Saez, A.; Dominguez, J. (1994): Comparative study of free boundary element approaches to transient dynamic crack problems. *Engn. Anal. Boundary Elem.*, 13: 11-19.

Cole, D. M.; Kosloff, D. D.; Minster, J. B. (1978): A numerical boundary integral method for elastodynamics. *Bull. Seismol. Soc. America*, 68: 1331-1357.

Cruse, T. A.; Rizzo, F. J. (1968): A direct formulation and numerical solution of the general elastodynamic problem. *J. Appl. Math. Analysis Appl.*, 22: 244-259.

Davies, B.; Martin, B. (1979): Numerical inversion of the Laplace transform: a survey and comparison of methods. *J. Comput. Phys.*, 33: 1-32.

Dominguez, J. (1993): Boundary Elements in Dynamics, CMP, Southampton.

Fedelinski, P.; Aliabadi, M. H.; Rooke, D. P. (1993): Dual boundary element method in dynamic fracture mechanics. *Engn. Anal. Boundary Elem.*, 12: 203-210.

Kögl, M.; Gaul, L. (2000): A 3-D boundary element method for dynamic analysis of anisotropic elastic solids. *CMES: Computer Modeling in Engineering & Sciences*, 1: 27-44.

Manolis, G. D.; Beskos, D. E. (1981): Dynamic stress concentration studies by boundary integrals and Laplace transform. *Int. J. Num. Meth. Engn.* 17: 573-599.

Manolis, G. D.; Beskos, D. E. (1988): Boundary Element Methods in Elastodynamics. Unwin Hyman, London.

Manolis, G. D.; Pavlou, S. (2002): A Green's function for variable density elastodynamics under plane strain conditions by Hormander's method. *CMES: Computer Modeling in Engineering & Sciences* 3: 399-416.

Mansur, W. J. (1983): A time-stepping technique to solve wave propagation problems using boundary element methods. Ph.D. Thesis, University of Southampton U.K.

Martin, P. A.; Richardson, J. D.; Gray, L. J.; Berger, J. R. (2002): On Green's function for a three-dimensional exponentially-graded elastic solid. Proc. R. Soc. London A 458: 1931-1947.

Mikhailov, S. E. (2002): Localized boundary-domain integral formulations for problems with variable coefficients. *Engn. Anal. Bound. Elem.*, 26: 681-690.

Nardini, D.; Brebbia, C. A. (1983): A new approach to free vibration analysis using boundary elements. *Appl. Math. Modelling*, 7: 157-162.

Partridge, P. W.; Brebbia, C. A.; Wrobel, L. C. (1992): The Dual Reciprocity Boundary Element Method. CMP, Southampton.

Perez-Gavilan, J. J.; Aliabadi, M. H. (2000): Galerkin boundary element formulation with dual reciprocity for elastodynamics. *Int. J. Num. Meth. Engn.*, 48: 1331-1334.

Schanz, M.; Antes, H. (1997): Application of 'Operational Quadrature Methods' in time domain boundary element methods. *Meccanica*, 32: 179-186.

Sladek, V.; Sladek, J. (1984): Transient elastodynamic three-dimensional problems in cracked bodies. *Appl. Math. Modelling*, 8: 2-10.

Sladek, V.; Sladek, J.; Markechova, I. (1993): An advanced boundary element method for elasticity problems in nonhomogeneous media. *Acta Mechanica*, 97: 71-90.

Sladek, J.; Sladek, V.; Atluri, S. N. (2001): A pure

contour formulation for meshless local boundary integral equation method in thermoelasticity. *CMES: Computer Modeling in Engineering & Sciences*, 2: 423-434.

Sladek, J.; Sladek, V.; Atluri, S. N. (2000): Local boundary integral equation (LBIE) method for solving problems of elasticity with nonhomogeneous material properties. *Comput. Mech.*, 24: 456-462.

Sladek, J.; Sladek, V.; Van Keer, R. (2003): Meshless local boundary integral equation method for 2D elastodynamic problems. *Int. J. Num. Meth. Engn.*, 57: 235-249.

Stehfest, H. (1970): Algorithm 368: numerical inversion of Laplace transform. *Comm. Assoc. Comput. Mach.*, 13: 47-49.

Sutradhar, A.; Paulino, G. H.; Gray, L. J. (2002): Transient heat conduction in homogeneous and non-homogeneous materials by the Laplace transform Galerkin boundary element method. *Engn. Anal. Boundary Elem.*, 26: 119-132.

Zhang, Ch.; Sladek, J.; Sladek, V. (2003a): Effects of material gradients on transient dynamic mode III SIFs in an FGM. *Int. J. Solids Struct.*, 40: 5251-5270.

Zhang, Ch.; Sladek, J.; Sladek, V. (2003b): Numerical analysis of cracked functionally graded materials. Key Engineering Materials, 251-252: 463-471.

Zhu, T. D.; Zhang, J. D.; Atluri, S. N. (1998a): A local boundary integral equation (LBIE) method in computational mechanics and a meshless discretization approach. *Comput. Mech.*, 21: 223-235.

Zhu, T. D.; Zhang, J. D.; Atluri, S. N. (1998b): A meshless local boundary integral equation (LBIE) method for solving nonlinear problems. *Comput. Mech.*, 22: 174-186.

Zhu, T. D.; Zhang, J. D.; Atluri S. N. (1999): A meshless numerical method based on the local boundary integral equation (LBIE) to solve linear and nonlinear boundary value problems. 21: 223-235. *Engn. Anal. Boundary Elem.*, 23: 375-390.